

Airy-Bessel wave packets as versatile linear light bullets

Andy Chong^{1*}, William H. Renninger¹, Demetrios N. Christodoulides² and Frank W. Wise¹

The generation of spatiotemporal optical wave packets that are impervious to both dispersion and diffraction has been a fascinating challenge¹. Despite intense research activity, such localized waves, referred to as light bullets, have remained elusive. In nonlinear propagation, three-dimensional light bullets tend to disintegrate as a result of inherent instabilities^{2,3}. Three-dimensional wave packets that propagate linearly have been reported^{4–9}, but their utility is severely limited by the need to tailor the wave packet precisely to material properties. To overcome these limitations, we explore a new approach based on the one-dimensional Airy wave packet¹⁰. Here, we report the first observation of a class of versatile three-dimensional linear light bullets, which combine Bessel beams in the transverse plane with temporal Airy pulses. Their evolution does not depend critically on the material in which they propagate, and the consequent versatility will facilitate their study and applications ranging from bioimaging¹¹ to plasma physics¹².

Any localized wave packet tends to broaden in space and time under the combined actions of diffraction and dispersion, which are universal physical processes¹. Methods to overcome the often undesirable consequences of these two effects have been pursued since the early days of lasers. In 1990, Silberberg proposed the use of self-action nonlinearities to simultaneously arrest dispersion and diffraction³. In this regime, light bullets correspond to three-dimensional (3D) solitons, propagation-invariant solutions of their respective evolution equations with particle-like properties. A major challenge arises from the fact that a single nonlinear process is responsible for balancing two linear effects simultaneously. These self-trapped bullets can only exist as ‘spherical’ spatiotemporal entities, that is, only when the effects of diffraction and dispersion are exactly equal². In addition, the ultrafast electronic nonlinearity responsible for self-focusing is supercritical, so 3D soliton bullets are by nature highly unstable; the wave packet either disperses or disintegrates during propagation¹³. As a consequence of these issues, 3D optical solitons have never been produced, and the generation of stable spatiotemporal solitons in even two-dimensional (2D) settings is achieved only in specific materials and with complicated experimental arrangements¹⁴. Nonlinear approaches generally require very high peak powers, which add to the challenge and will be undesirable in possible applications in which delicate materials such as biological tissue are to be probed. Thus, although the generation of 3D spatiotemporal solitons is a major scientific goal, we are motivated to consider other 3D localized waves.

Linear optics may provide an alternative route to the realization of 3D light bullets. Several diffraction/dispersion-free field configurations have been identified, with the Bessel beam^{15,16} perhaps being the best known. Non-diffracting beams can propagate over many Rayleigh lengths without any appreciable change in their intensity profiles. This property is used in applications such as optical

tweezing¹⁷, the generation of plasma channels¹⁸, material modification¹⁹ and microlithography²⁰. The availability of 3D localized wave packets would extend this list to settings that benefit from invariant temporal profiles. For example, a 3D light bullet is evidently the ideal field configuration for recently developed optical projection tomography, which has the potential to image to much greater depths than confocal microscopy²¹. If the group-velocity dispersion is normal (anomalous), linear light bullets in the form of X-waves^{6,7} (O-waves^{8,9}) are possible. Like their soliton counterparts, these waves can only exist if the diffraction and dispersion lengths are equal. In addition, the space and time variables are intertwined in these solutions, which makes their synthesis challenging. Sophisticated techniques for coupling the temporal (spectrum) and spatial (cone angle) profiles underlie the invariant propagation of the so-called Bessel-X pulses⁵. Clearly, sufficiently detailed knowledge of the optical properties of the propagation medium is a prerequisite to the generation of such 3D states. The only way to circumvent this problem is to disengage space and time.

Separation of the 3D spatiotemporal problem into elemental constituents requires at least one one-dimensional (1D) dispersion/diffraction-free wave packet. Such non-dispersing solutions do exist in the form of Airy functions, and in fact the Airy functions are unique: they are the only possible dispersion-free solutions in one dimension^{22,23}. It is only recently that Airy beams have been realized in optics^{10,24}.

In this Letter we report the generation of Airy-Bessel wave packets, first envisioned theoretically in ref. 24, that propagate without spreading despite diffraction and dispersion. Temporal self-healing and free acceleration, which are signatures of these wave packets, are demonstrated. These spatiotemporal waves are possible for either sign of dispersion and do not require equalization of diffraction and dispersion. This class of robust and versatile waves can be used in ultrafast probing or imaging in media with poorly known or dynamically varying properties.

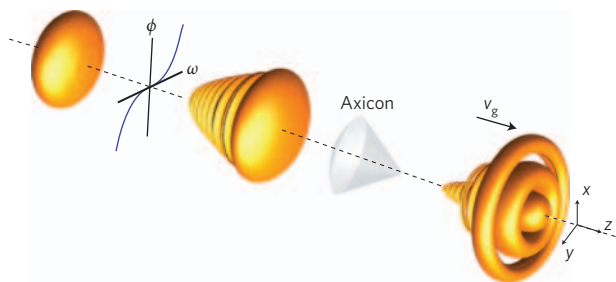


Figure 1 | Experimental schematic. 3D plots comprising iso-intensity contour plots of Gaussian-Gaussian (initial profile), Airy-Gaussian (after adding a large cubic spectral phase) and Airy-Bessel (after the axicon) wave packets. ϕ , ω and v_g are phase, optical frequency and group velocity, respectively.

¹Department of Applied Physics, Cornell University, Ithaca, New York 14853, USA, ²College of Optics/CREOL, University of Central Florida, Orlando, Florida 32816, USA. *e-mail: cyc26@cornell.edu

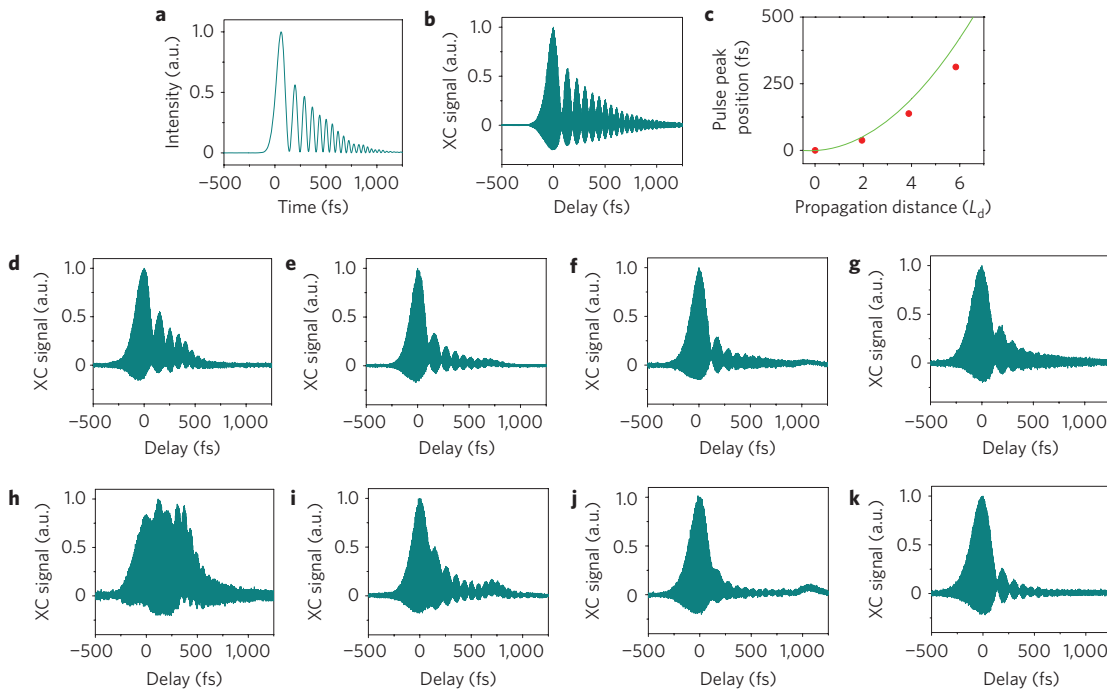


Figure 2 | Non-dispersive propagation, free acceleration and self-healing of an Airy pulse. **a**, Theoretical Airy pulse. **b**, Cross-correlation (XC) of the theoretical pulse with a reference pulse. **c**, Measured (symbols) and theoretical (line) temporal shift of the peak of the Airy pulse with propagation. **d–g**, The Airy pulse after dispersive propagation through 0 (**d**), 2 (**e**), 4 (**f**) and 6 (**g**) dispersion lengths (L_d). **h–k**, Self-healing of the Airy pulse: injured Airy pulse (**h**); gradual healing of its peak at 2 (**i**), 4 (**j**) and 6 (**k**) L_d .

The equation that governs the linear spatiotemporal evolution of an optical field E is

$$i\frac{\partial E}{\partial z} + \frac{1}{2k}\left(\frac{\partial^2 E}{\partial x^2} + \frac{\partial^2 E}{\partial y^2}\right) - \frac{k_o''}{2}\frac{\partial^2 E}{\partial \tau^2} = 0 \quad (1)$$

where z is the propagation axis and $\tau = t - (z/v_g)$ is time in a reference frame moving at the group velocity v_g of the wave. The second term in equation (1) accounts for diffraction, and the last term describes dispersion. $k = \omega_o n(\omega_o)/c$ (n is the index of refraction, c is the speed of light, and ω_o is the centre frequency) is the wave number and $k_o'' = \partial^2 k / \partial \omega^2$ is the dispersion coefficient of the medium evaluated at ω_o . Equation (1) admits an invariant, separable solution with intensity profile²⁴

$$I(r, z) = I_0 J_0^2(r/r_o) A_i^2 \left[\varepsilon \frac{\tau}{\tau_o} - \frac{(k_o'')^2 z^2}{4\tau_o^4} \right] \quad (2)$$

I_0 is the peak intensity, $J_0(x)$ and $A_i(x)$ are Bessel and Airy functions respectively, $r = \sqrt{x^2 + y^2}$, $\varepsilon = \pm 1$ determines the direction of the Airy function envelope, and r_o and τ_o determine the radial and temporal widths of the wave packet, respectively. An iso-intensity contour of this wave is shown in Fig. 1. Unlike other types of self-localized waves, these bullets exist without dispersion/diffraction equalization (that is, for any values of r_o and τ_o) and for either normal ($k_o'' > 0$) or anomalous ($k_o'' < 0$) dispersion. The bullet can be launched with its main lobe at the front ($\varepsilon = -1$, as in Fig. 1), in which case it will accelerate in time, or tail-first ($\varepsilon = 1$), in which case it will decelerate. Other families of localized solutions are possible. These include Airy temporal packets coupled with other 2D non-diffracting beams (higher-order Bessel or Mathieu beams, and so on^{4,25}) or even an Airy–Airy–Airy configuration. These wave packets will require more complicated arrangements than the single optic used to produce a Bessel beam, but they may

have interesting and useful features. For example, the Airy–Airy–Airy wave packet will follow a curved trajectory, which may be useful for some applications²⁶.

Techniques for producing Bessel beams are established¹⁵, so we first address the temporal profile. The creation of an Airy beam or pulse relies on the fact that the Fourier transform of the exponentially apertured Airy function is a Gaussian amplitude spectrum with a cubic phase, $\psi(\omega) \approx \exp(-\alpha\omega^2)\exp(i\beta\omega^3)$, where α determines the spectral bandwidth and β determines the cubic phase¹⁰. We find that a grating-telescope combination in a standard configuration for controlling group-velocity dispersion offers a simple and convenient way to impress the required spectral phase on a short light pulse. A fibre laser generates a broadband spectrum with a large quadratic spectral phase. A small portion of this pulse is split off and compressed to the Fourier-transform limit of ~ 50 fs, for use as a reference pulse in measurements. A grating-telescope combination compensates the quadratic spectral phase completely, and impresses an adjustable cubic phase on the main pulse, to create the Airy profile.

The intriguing features of the Airy pulse are revealed by recording the cross-correlation with the reference pulse after various propagation distances. Figure 2a, b shows the Airy pulse and the theoretical cross-correlation, respectively. The synthesized Airy pulse (Fig. 2d) consists of a main lobe of duration ~ 100 fs, followed by a series of smaller peaks. By inverting the sign of the cubic phase, an Airy pulse with the smaller peaks preceding the main lobe ($\varepsilon = 1$) can also be created. Figure 2e–g shows the profiles of the Airy packet after propagation through 25, 50 and 75 cm of silicate glass (BK7). The main lobe is almost invariant over this range. These distances correspond to 2, 4 and 6 characteristic dispersion lengths ($L_d = \tau_o^2/k_o''$, where τ_o is the half-width at $1/e$ -maximum pulse duration), so a Gaussian pulse with the duration of the main lobe would have broadened by a factor of 6 in the same propagation distance. Note that, without the cubic phase being impressed on the broad spectrum, the pulse would broaden by a factor of 24 after propagation through

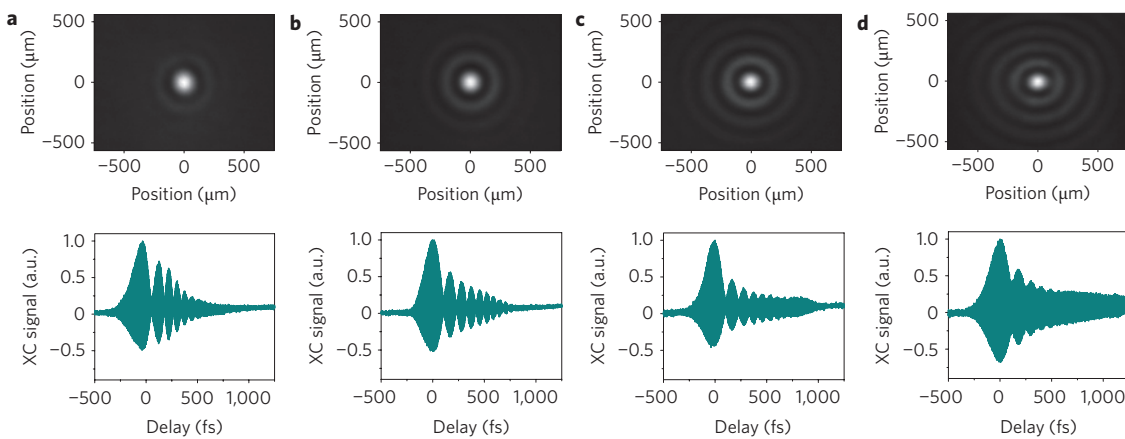


Figure 3 | Propagation of an Airy-Bessel bullet. **a**, Initial spatial and temporal profiles. **b-d**, Profiles after propagation through 3.3 diffraction lengths, L_R , and 1.8 dispersion lengths, L_d (**b**), 5.4 L_R and 3.6 L_d (**c**) and 7.5 L_R and 5.4 L_d (**d**). L_R is the diffraction length of a beam with a diameter of 180 μm, and L_d is the dispersion length of a 100-fs pulse.

the same distance. These features are observed irrespective of whether the Airy pulse experiences normal or anomalous dispersion. A noteworthy property of Airy packets is their ability to accelerate freely during propagation without violating Ehrenfest's momentum theorem²³. Spatial acceleration was recently used in the production of curved plasma channels²⁶. To study their temporal acceleration, the Airy and reference pulses were arranged to propagate collinearly through the glass. The Airy pulse was delayed by 2 ps with respect to the reference pulse, and the relative delay between the pulses was recorded versus propagation distance in the glass. The peak of the Airy pulse follows a parabolic trajectory in time, as expected theoretically (Fig. 2c). The acceleration refers to the local features of the pulse; the temporal position of its centroid is invariant. Finally, Airy wave packets exhibit remarkable ‘self-healing’ after distortion^{27,28}. Because its duration is only ~100 fs, it is technically difficult to modulate the Airy pulse in the time domain. Intuitively, the cubic phase delays both the low- and high-frequency components of the pulse, so the central part of the spectrum corresponds to the main temporal lobe. By filtering out the centre of the spectrum, the main temporal peak can be selectively attenuated to ‘injure’ the packet (Fig. 2h). The main peak and the overall pulse shape are restored during the propagation through 25–75 cm of glass (Fig. 2i–k). The secondary pulses serve as an energy reservoir to restore the primary lobe of the Airy packet. These measurements clearly demonstrate the key features of the Airy pulse.

To obtain the Airy-Bessel wave packet, we then convert the spatial wavefront into a Bessel beam. The output of the fibre laser is a pristine Gaussian beam approximately 1 mm in diameter, which is unaffected by the conversion to the Airy temporal profile. The Airy-Gaussian beam was converted to an Airy-Bessel wave packet by a beam-expansion telescope and an axicon lens²⁹ with 179° apex angle (Fig. 1; see Supplementary Fig. S1).

The propagation of the Airy-Bessel wave packet through a glass with large refractive index and dispersion (Schott SF14, Corning; see Supplementary Information) was monitored simultaneously by cross-correlation for the time profile and a charge-coupled device (CCD) camera for the spatial distribution. The profiles of the initial Airy-Bessel wave packet are shown in Fig. 3a. The diameter of the central lobe is ~180 μm, and the pulse duration is ~100 fs. Figure 3b, c shows that the spatiotemporal profile is maintained after propagation through 5, 10 and 15 cm in the glass, respectively. A single pass through the glass sample corresponds to 1.3 diffraction lengths ($L_R = \pi n r_o^2 / \lambda$, where r_o is the beam radius, n is the index of refraction and λ is the wavelength) and 1.8 dispersion lengths, with additional ~1.2 diffraction length

contribution from the free space propagation to the CCD camera. Thus, a wave packet with Gaussian spatial and temporal profiles corresponding to the main lobe of the Airy-Bessel wave packet would have broadened by a factor of 7.5 in space and 5.5 in time after passage through 15 cm of glass. The intensity of the corresponding Gaussian pulse/beam would fall by a factor of ~250. In addition, these results illustrate an important feature of these linear light bullets: there is no need to precisely tailor the dispersion and diffraction lengths. The flexibility that is possible in producing these linear bullets will undoubtedly facilitate their use in applications. Fundamentally, the Airy-Bessel wave packet in Fig. 3 can have ~10% of the energy of the original Gaussian-Gaussian wave packet in the main spatiotemporal lobe. The energy required to synthesize the Airy-Bessel packet may be a limitation for some applications.

The specific role of the Airy temporal profile can be illustrated by visualizing the propagation of the Airy-Bessel bullet through a dispersive and fluorescent medium consisting of Rhodamine B dye molecules dissolved in a solution of carbon disulphide (see Supplementary Information). A cuvette with a path length of 10 cm in CS₂ corresponds to three dispersion lengths. Because the two-photon-excited fluorescence depends nonlinearly on the square of intensity, the fluorescence trace constitutes a sensitive diagnostic of the peak intensity. As a control experiment, the fluorescence channel generated by the corresponding Gaussian-Bessel pulse was recorded (Fig. 4a), as in ref. 30. The non-diffracting nature of the Bessel beam is evident, but the fluorescence decays after ~5 cm of propagation owing to dispersive broadening of the pulse. At the end of the cuvette, the fluorescence excited by the

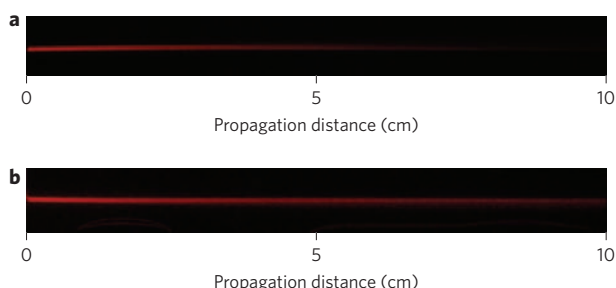


Figure 4 | Two-photon-excited fluorescence in a dispersive Rhodamine-B dye solution. **a**, Gaussian-Bessel wave packet with a duration of ~120 fs and diameter of 180 μm. **b**, Airy-Bessel bullet with a main lobe pulse duration of ~120 fs and diameter of 180 μm.

Airy–Bessel packet is approximately five times more intense than the fluorescence from the Gaussian–Bessel packet. This implies that the Gaussian–Bessel packet spreads two to three times more than the Airy–Bessel pulse, as expected.

In summary, we have generated localized optical wave packets that propagate without broadening in time or space. The production of these light bullets does not depend on detailed knowledge of material properties, which will allow them to be truly versatile as probes of light–matter interactions as well as in a broad range of applications.

Received 13 October 2009; accepted 26 November 2009;
published online 17 January 2010

References

1. Saleh, B. E. A. & Teich, M. C. *Fundamentals of Photonics* 2nd edn (Wiley, 2007).
2. Malomed, B. A., Mihalache, D., Wise, F. & Torner, L. Spatiotemporal solitons. *J. Opt. B* **7**, R53–R72 (2005).
3. Silberberg, Y. Collapse of optical pulses. *Opt. Lett.* **15**, 1282–1284 (1990).
4. Hernández-Figueroa, H. E., Zamboni-Rached, M. & Recami, E. *Localized Waves* (John Wiley & Sons, 2008).
5. Sönajalg, H., Rätsep, M. & Saari, P. Demonstration of the Bessel-X pulse propagation with strong lateral and longitudinal localization in a dispersive medium. *Opt. Lett.* **22**, 310–312 (1997).
6. Lu, J. Y. & Greenleaf, J. F. Nondiffracting X-waves. Exact solutions to free space scalar wave equation and their finite aperture realizations. *IEEE Trans. Ultrason. Ferroelec. Freq. Cont.* **39**, 19–31 (1992).
7. Di Trapani, P. *et al.* Spontaneously generated X-shaped light bullets. *Phys. Rev. Lett.* **91**, 093904 (2003).
8. Porras, M. A. & Di Trapani, P. Localized and stationary light wave modes in dispersive media. *Phys. Rev. E* **69**, 066606 (2004).
9. Longhi, S. Localized subluminal envelope pulses in dispersive media. *Opt. Lett.* **29**, 147–149 (2004).
10. Siviloglou, G. A., Broky, J., Dogariu, A. & Christodoulides, D. N. Observation of accelerating Airy beams. *Phys. Rev. Lett.* **99**, 213901 (2007).
11. Brown, C. T. A. *et al.* Enhanced operation of femtosecond lasers and applications in cell transfection. *J. Biophoton.* **1**, 183–199 (2008).
12. Kruer, W. *The Physics of Laser Plasma Interactions* (Westview Press, 2003).
13. Rasmussen, J. J. & Rydal, K. Blow-up in nonlinear Schrödinger equations. *Phys. Scr.* **33**, 481–497 (1986).
14. Liu, X., Qian, L. J. & Wise, F. W. Generation of optical spatiotemporal solitons. *Phys. Rev. Lett.* **82**, 4631–4634 (1999).
15. Durnin, J., Miceli, J. J. & Eberly, J. H. Diffraction-free beams. *Phys. Rev. Lett.* **58**, 1499–1501 (1987).
16. Gori, F., Guattari, G. & Padovani, C. Bessel-Gauss beams. *Opt. Commun.* **64**, 491–495 (1987).
17. Garcez-Chavez, V. *et al.* Simultaneous micromanipulation in multiple planes using a self-reconstructing light beam. *Nature* **419**, 145–147 (2002).
18. Fan, J., Parra, E. & Milchberg, H. M. Resonant self-trapping and absorption of intense Bessel beams. *Phys. Rev. Lett.* **84**, 3085–3088 (2000).
19. Amako, J., Sawaki, D. & Fujii, E. Microstructuring transparent materials by use of non-diffracting ultrashort pulse beams generated by diffractive optics. *J. Opt. Soc. Am. B* **20**, 2562–2568 (2003).
20. Erdelyi, M. *et al.* Generation of diffraction-free beams for applications in optical microlithography. *J. Vac. Sci. Technol. B* **15**, 287–292 (1997).
21. Sharpe, J. *et al.* Optical projection tomography as a tool for 3D microscopy and gene expression studies. *Science* **296**, 541–545 (2002).
22. Berry, M. V. & Balazs, N. L. Nonspreadng wave packets. *Am. J. Phys.* **47**, 264–267 (1979).
23. Besieris, I. M. & Shaarawi, A. M. A note on accelerating finite energy Airy beam. *Opt. Lett.* **32**, 2447–2449 (2007).
24. Siviloglou, G. A. & Christodoulides, D. N. Accelerating finite energy Airy beams. *Opt. Lett.* **32**, 979–981 (2007).
25. Gutiérrez-Vega, J. C., Iturbe-Castillo, M. C. & Chávez-Cerda, S. Alternative formulation for invariant optical fields: Mathieu beams. *Opt. Lett.* **25**, 1493–1495 (2000).
26. Polynkin, P. *et al.* Curved plasma channel generation using ultraintense Airy beams. *Science* **324**, 229–232 (2009).
27. Broky, J., Siviloglou, G. A., Dogariu, A. & Christodoulides, D. N. Self-healing properties of optical Airy beams. *Opt. Express* **16**, 12880–12891 (2008).
28. Baumgartl, J., Mazilu, M. & Dholakia, K. Optically mediated particle clearing using Airy wavepackets. *Nature Photon.* **2**, 675–678 (2008).
29. Scott, G. & McArdle, N. Efficient generation of nearly diffraction-free beams using an axicon. *Opt. Eng.* **31**, 2640–2643 (1992).
30. Polesana, P. *et al.* High localization, focal depth and contrast by means of nonlinear Bessel beams. *Opt. Express* **13**, 6160–6167 (2005).

Acknowledgements

The authors thank A. Bartnik and K. Kieu for their help. This work was supported by the National Science Foundation (PHY-0653482).

Author contributions

A.C. performed the experiments and analysed the data. W.H.R. performed a theoretical study with some numerical simulations. D.N.C. proposed the original concept and analytic models. F.W.W. supervised the project. The manuscript was prepared by A.C., D.N.C. and F.W.W.

Additional information

The authors declare no competing financial interests. Supplementary information accompanies this paper at www.nature.com/naturephotronics. Reprints and permission information is available online at <http://npg.nature.com/reprintsandpermissions/>. Correspondence and requests for materials should be addressed to A.C.